ROYAL SOCIETY
OF CHEMISTRY

PAPER

Atmospheric protein chemistry influenced by anthropogenic air pollutants: nitration and oligomerization upon exposure to ozone and nitrogen dioxide†

Fobang Liu,[a] Pascale S. J. Lakey,[a] Thomas Berkemeier,[ab]
Haijie Tong, [ID][a] Anna Theresa Kunert,[a] Hannah Meusel,[a]
Yafang Cheng,[a] Hang Su,[a] Janine Fröhlich-Nowoisky,[a] Senchao Lai,[c]
Michael G. Weller,[d] Manabu Shiraiwa,[e] Ulrich Pöschl[a]
and Christopher J. Kampf [ID] *[af]

The allergenic potential of airborne proteins may be enhanced *via* post-translational modification induced by air pollutants like ozone (O_3) and nitrogen dioxide (NO_2). The molecular mechanisms and kinetics of the chemical modifications that enhance the allergenicity of proteins, however, are still not fully understood. Here, protein tyrosine nitration and oligomerization upon simultaneous exposure of O_3 and NO_2 were studied in coated-wall flow-tube and bulk solution experiments under varying atmospherically relevant conditions (5–200 ppb O_3, 5–200 ppb NO_2, 45–96% RH), using bovine serum albumin as a model protein. Generally, more tyrosine residues were found to react *via* the nitration pathway than *via* the oligomerization pathway. Depending on reaction conditions, oligomer mass fractions and nitration degrees were in the ranges of 2.5–25% and 0.5–7%, respectively. The experimental results were well reproduced by the kinetic multilayer model of aerosol surface and bulk chemistry (KM-SUB). The extent of nitration and oligomerization strongly depends on relative humidity (RH) due to moisture-induced phase transition of proteins, highlighting the importance of cloud

[a]Multiphase Chemistry Department, Max Planck Institute for Chemistry, Hahn-Meitner-Weg 1, 55128 Mainz, Germany

[b]School of Chemical & Biomolecular Engineering, Georgia Tech, Atlanta, GA, USA

[c]School of Environment and Energy, South China University of Technology, Higher Education Mega Center, Guangzhou 510006, P. R. China

[d]Division 1.5 Protein Analysis, Federal Institute for Materials Research and Testing (BAM), Richard-Willstätter-Str. 11, 12489 Berlin, Germany

[e]Department of Chemistry, University of California, Irvine, CA, USA

[f]Institute for Organic Chemistry, Johannes Gutenberg University Mainz, Duesbergweg 10-14, 55128 Mainz, Germany. E-mail: kampfc@uni-mainz.de

† Electronic supplementary information (ESI) available: Chemical mechanism and corresponding parameters used in kinetic modelling (Table S1), schematic experimental setup (Fig. S1), and SEC calibration curve (Fig. S2). See DOI: 10.1039/c7fd00005g

processing conditions for accelerated protein chemistry. Dimeric and nitrated species were major products in the liquid phase, while protein oligomerization was observed to a greater extent for the solid and semi-solid phase states of proteins. Our results show that the rate of both processes was sensitive towards ambient ozone concentration, but rather insensitive towards different NO_2 levels. An increase of tropospheric ozone concentrations in the Anthropocene may thus promote pro-allergic protein modifications and contribute to the observed increase of allergies over the past decades.

1.   Introduction

Allergies represent an important issue for human health and the prevalence of allergic diseases has been increasing worldwide over the past decades.[1,2] Among other explanations, air pollution has been proposed as a potential driver for this increase.[3–6] It is well established that air pollutants, especially diesel exhaust particles (DEPs), can act as adjuvants and facilitate allergic sensitization in the human body.[7,8] Air pollutants like nitrogen dioxide (NO_2), sulfur dioxide (SO_2), and ozone (O_3) have been shown to interact with and modify allergen carriers like pollen grains and fungal spores, increasing the release of allergenic proteins.[8,9] Moreover, post-translational modifications (PTM) of allergenic proteins can be induced by reactive trace gases such as O_3 and NO_2 which modifies their structure and activity, thus altering the immunogenicity of the proteins.[10–13]

Airborne allergenic proteins (aeroallergens) are contained not only in coarse biological particles such as pollen grains,[14] but also in the fine fraction of air particulate matter (aerodynamic diameter < 2.5 μm).[15–17] The occurrence of allergenic proteins in fine particles can be explained by several processes, including the release of pollen cytoplasmic granules (PCGs) from the rupture of pollen grains,[9] fragmentation of airborne cellular material,[18] and contact transfer of allergenic proteins onto fine particles.[18,19] Therefore, aeroallergens can be directly exposed to ambient O_3 and NO_2, promoting chemical modifications like tyrosine (Tyr) nitration and oligomerization.

Laboratory and field investigations have shown that proteins can be oxidized, nitrated and/or oligomerized upon exposure to NO_2 and O_3 in synthetic gas mixtures or polluted urban air.[11,12,15,20] The mechanisms of protein nitration by O_3 and NO_2, and protein cross-linking (oligomerization) by O_3 both involve the formation of long-lived reactive oxygen intermediates (ROIs), which are most likely tyrosyl radicals, as proposed earlier.[12,20–24] The ROIs can subsequently react with each other forming dityrosine (DTyr) crosslinks with NO_2 to form nitro-tyrosine (NTyr) residues, or undergo further oxidation reactions. Using quantum chemical methods, Sandhiya et al.[22] showed that six different intermediates can be formed through the initial oxidation of Tyr residues by O_3, out of which the tyrosyl radical is favorable due to a small energy barrier, particularly in the aqueous phase. In the absence of NO_2, tyrosyl radicals can undergo self-reaction to stabilize in the form of dimers. Under physiological conditions, Pfeiffer et al.[25] found that DTyr was a major product of Tyr modification caused by low steady-state concentrations of peroxynitrite, while high fluxes (>2 μM s^{-1}) of nitrogen oxide/superoxide anions (NO/O_2^-) are required to render peroxynitrite an efficient trigger of Tyr nitration. Thus, kinetic competition between Tyr nitration and dimerization (or oligomerization) upon protein exposure to O_3 and NO_2 can be

expected, which needs to be explored in detail to assess the relevant atmospheric conditions that favor potentially health relevant protein modifications.

In this study, we explored the oxidation, nitration, and oligomerization reactions of proteins induced by O_3 and NO_2, and their kinetics under different atmospherically relevant conditions using bovine serum albumin (BSA) as a model protein. Coated-wall flow-tube and bulk solution experiments were performed to study the kinetics of protein nitration and oligomerization at O_3 and NO_2 concentrations of 5–200 ppb, and relative humidities (RH) of 45% and 96%, utilizing a size exclusion chromatography/spectrophotometry method. Additionally, we used the kinetic multilayer model of aerosol surface and bulk chemistry (KM-SUB)[26] to investigate which chemical reactions and transport processes control the concentration and time dependence of protein oligomerization and nitration.

2. Experimental

2.1. Materials

Bovine serum albumin (BSA, A5611) and sodium phosphate monobasic monohydrate ($NaH_2PO_4 \cdot H_2O$, 71504), were purchased from Sigma Aldrich (Germany). Sodium hydroxide (NaOH, 0583) was purchased from VWR (Germany). $10\times$ Tris/glycine/SDS (161-0732) was purchased from Bio-Rad Laboratories (USA). High purity water (18.2 MΩ cm) for chromatography was taken from a Milli-Q Integral 3 water purification system (Merck Millipore, USA). The high purity water (18.2 MΩ cm) was autoclaved before use if not specified otherwise.

2.2. Protein O_3/NO_2 exposure setup

Reactions of BSA with O_3/NO_2 mixtures were performed both homogeneously in aqueous solutions and heterogeneously *via* the exposure of BSA-coated glass tubes to gaseous O_3/NO_2 at different levels of relative humidity (RH). Before the exposure experiments, BSA solutions (0.6 mL, 0.33 mg mL^{-1}) were loaded into the glass tube and dried by passing a nitrogen (N_2, 99.999%) flow at $\sim$1 L min^{-1} through a specific rotating device,[27] which is essential to ensure homogeneous coating and experiment reproducibility. The BSA-coated glass tube was then connected to the experimental setup. The experimental setup (Fig. S1, ESI†) was described previously,[20] and was extended by incorporating an additional flow of NO_2 after the humidifier.

Briefly, ozone was produced from synthetic air passed through a UV lamp (L.O.T.-Oriel GmbH & Co. KG, Germany) at $\sim$1.9 L min^{-1}. The gas flow was then split and one flow was passed through a Nafion® gas humidifier (MH-110-12F-4, PermaPure, USA) operated with autoclaved high purity water, while the other flow remained dry. RH could be varied in a wide range by adjusting the ratio between the dry and humidified air flow. During the experiments, the standard deviation from the set RH values was <2% RH. The gas flow with a set O_3 concentration and RH was then mixed with a N_2 flow containing $\sim$5 ppmV NO_2 (Air Liquide, Germany). The NO_2 concentrations were adjusted by varying the flow rate (20–80 mL min^{-1}) of the $\sim$5 ppmV NO_2 flow. The combined gas flow was then directed through the BSA-coated glass tube. The concentrations of O_3 and NO_2 as well as RH were measured using commercial monitoring instruments (Ozone analyzer,

49i, Thermo Scientific, Germany; NO_x analyzer, 42i-TL, Thermo Scientific, Germany; RH sensor FHA 646-E1C with ALMEMO 2590-3 instrument, Ahlborn, Mess- und Regelungstechnik, Germany). After exposure, the proteins were extracted from the glass tube with 1.5 mL of 1× Tris/glycine/SDS (pH 8.3) buffer to avoid precipitation of protein oligomers in the extract solution.

For homogeneous bulk solution reactions, the O_3/NO_2 gas mixtures were directly bubbled through 1.5 mL of 0.13 mg mL^{-1} BSA aqueous solutions (pH 7.0 ± 0.2; measured by a pH meter, model WTW multi 350i, WTW, Germany) at a flow rate of 60 mL min^{-1} using a Teflon tube (ID: 1.59 mm). All heterogeneous and homogeneous exposure experiments were performed in duplicate.

2.3. SEC-HPLC-DAD analysis

Product analysis was performed using high-performance liquid chromatography coupled to diode array detection (HPLC-DAD, Agilent Technologies 1200 series). The HPLC-DAD system consisted of a binary pump (G1379B), an autosampler with a thermostat (G1330B), a column thermostat (G1316B), and a photodiode array detector (DAD, G1315C). ChemStation software (Rev. B.03.01, Agilent) was used for system control and data analysis. Molecular weight (MW) separation by size exclusion chromatography (SEC) was carried out using an AdvanceBio SEC column (Agilent, 300 Å, 300 × 4.6 mm, 2.7 μm). Isocratic separation at a flow rate of 0.35 mL min^{-1} was carried out using a mobile phase of 150 mM NaH_2PO_4 buffer (adjusted to pH 7 with 10 M NaOH (aq)) after injecting 40 μL of sample. The absorbance was monitored by the DAD at wavelengths of 220, 280 and 357 nm. Each chromatographic run was performed in duplicate.

A protein standard mix 15–600 kDa (69385, Sigma Aldrich, Germany) containing bovine thyroglobulin (MW = 670 kDa), γ-globulin from bovine blood (MW = 150 kDa), chicken egg albumin, grade VI (MW = 44.3 kDa), and ribonuclease A (MW = 13.7 kDa) was used for SEC column calibration (elution time vs. log MW). Details can be found in Fig. S2 in the ESI.† It should be noted that SEC separates molecules according to their hydrodynamic sizes, thus only approximate molecular masses can be obtained by this calibration method.

2.4. Determination of protein oligomer mass fractions and nitration degrees

A detailed description of the simultaneous determination of protein oligomer mass fractions and nitration degrees using the SEC-HPLC-DAD analysis described above can be found in Liu et al.[28] Briefly, we report the formation of BSA oligomers as the temporal evolution in the ratios of the respective oligomers (dimers, trimers, and oligomers with $n \geq 4$) to the sum of monomer and all oligomer peak areas at the absorption wavelength of 220 nm. Assuming that the molar extinction coefficients of the individual protein oligomer fractions are multiples of the monomer extinction coefficient, the calculated oligomer ratios correspond to the mass fractions (ω) of the individual oligomers. Nitration degrees (NDs), defined as the concentration of nitrotyrosine (NTyr) divided by the sum of the concentrations of NTyr and Tyr, were obtained for BSA monomers and dimers, using the respective peak areas of the monomer and dimer signals at wavelengths of 280 nm and 357 nm. For calculation of the total protein ND, the sum of the peak areas of all protein signals at wavelengths of 280 nm and 357 nm was used. Note that corresponding to the definition of the ND, the same number of nitrated Tyr

residues in a BSA monomer and dimer will lead to a factor of 2 difference in the individual NDs, because a BSA dimer contains twice the number of Tyr residues compared to the monomer. Further information on the calculation of NDs can be found in Liu *et al.*[28] The values and errors of the calculated NDs and oligomer mass fractions represent the arithmetic mean values and standard deviations of duplicate experiments.[29] The commercially available BSA also contains dimers and trimers of the protein as well as pre-nitrated monomers and dimers ($\sim$NDs 0.9%). Therefore, the reported values of oligomer mass fractions and NDs were corrected for these background signals.

3. Results and discussion

3.1. Protein oligomerization

Fig. 1 and 2 show the effects of varying NO_2 and O_3 concentrations on protein oligomerization for homogeneous bulk solution and coated-wall flow-tube experiments, respectively. Exposures were carried out at fixed NO_2
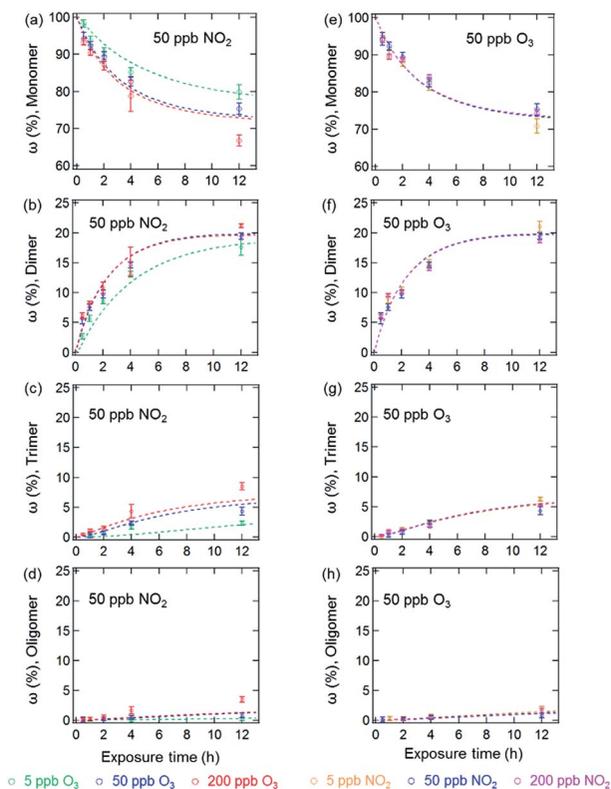

Fig. 1 Temporal evolution of protein oligomer mass fractions (ω (%), monomer, dimer, trimer and oligomer ($n \geq 4$)) in the aqueous phase reaction of BSA with O_3/NO_2: ((a)–(d)) at a fixed NO_2 concentration of 50 ppb with varied O_3 concentrations; ((e)–(h)) at a fixed O_3 concentration of 50 ppb with varied NO_2 concentrations. The data points and error bars represent the arithmetic mean values and standard deviations of duplicate experiments. The dashed lines are the results of the kinetic model.
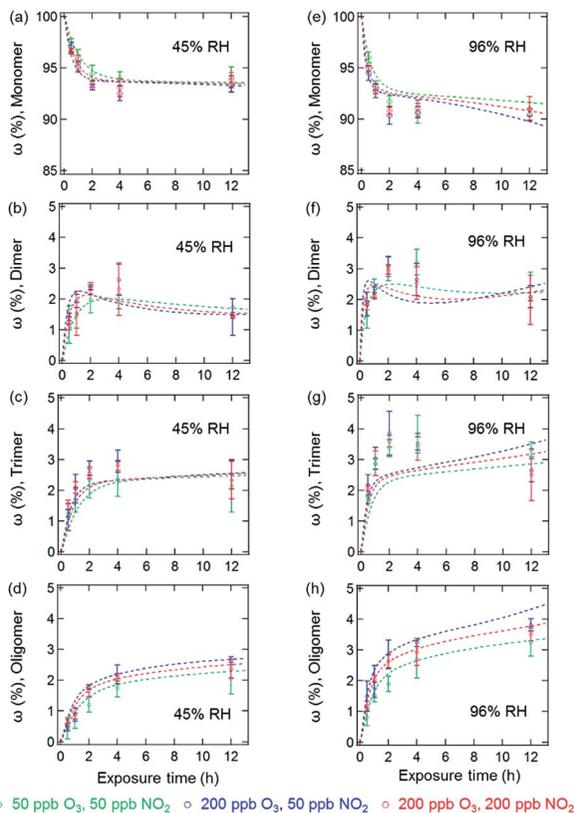
Fig. 2 Temporal evolution of protein oligomer mass fractions (ω (%), monomer, dimer, trimer and oligomer ($n \geq 4$) upon exposure of BSA films (thickness 34 nm) to various O_3/NO_2 concentrations: ((a)–(d)) at 45% RH; ((e)–(h)) at 96% RH. The data points and error bars represent the arithmetic mean values and standard deviations of duplicate experiments. The dashed lines are the results of the kinetic model.

concentrations with varying O_3 concentrations and *vice versa*. The exposure time was varied from 0.5 up to 12 h. While in bulk solution experiments dimers were generally observed as the major reaction products of BSA with O_3 and NO_2, trimers or higher oligomers can be dominant products in the coated-wall flow-tube experiments at longer exposure times, depending on the experimental conditions.

The results of the bulk solution experiments on protein oligomerization are illustrated in Fig. 1. Generally, the mass fractions of dimers, trimers, and higher oligomers increase with increasing reaction times, reaching up to 21 ± 1% for dimers, 9 ± 1% for trimers, and 4 ± 1% for oligomers with $n \geq 4$ after 12 h of exposure. The minimum mass fraction of monomers correspondingly was found to be 66%. While varying the O_3 concentrations (Fig. 1a–d, fixed 50 ppb of NO_2) from 5 to 200 ppb significantly affected the temporal evolutions observed for the mass fractions of the different oligomers, changing the NO_2 concentration (Fig. 1e–h, fixed 50 ppb of O_3) in the same range did not result in significant changes in oligomer mass fractions. The solubility of O_3 and NO_2 in water is

$\sim 10^{-5}$ mol mL^{-1} (derived from their Henry's law constants: $K_{sol,cc,O_3} \approx K_{sol,cc,NO_2}$ $\approx 10^{-2}$ M atm^{-1})[30] under our experimental conditions. Increasing O_3 and NO_2 gas concentrations between 5 to 200 ppb should result in concentrations of O_3 and NO_2 between 7×10^{-11} to 3×10^{-9} M in the aqueous phase. Thus, the insignificant change of oligomer mass fractions with varied NO_2 concentration should not be caused by a saturation of dissolved NO_2 in the concentration range investigated (5 to 200 ppb).

Mechanistically, the reactions between O_3/NO_2 and protein Tyr residues involve the formation of ROIs (tyrosyl radicals) resulting from the reaction of Tyr with O_3. These ROIs can then either react with NO_2 to form NTyr residues or cross-link due to intermolecular DTyr formation.[6,20] Ozonolysis of Tyr may also result in other oxidized products such as 3,4-dihydroxyphenylalanine (DOPA).[31] However, the reaction mechanism for the formation of these oxidized products is not the focus of this study and we only consider these modified Tyr derivatives in the proposed mechanism (Table S1†) as a portion of the oxidized amino acid residues. Regardless, an inhibition of intermolecular DTyr cross-linking would be expected with increasing NO_2 concentrations. However, no such behavior was observed. Furthermore, similar protein oligomer mass fractions were observed previously in the absence of NO_2 for BSA exposed to O_3 in bulk solution experiments with comparable levels of O_3 (50 and 200 ppb).[20] This observation may be due to the high number of accessible Tyr residues on the dissolved BSA molecules in solution, because after 12 h of exposure, 66% of BSA (Fig. 1a) is still present in monomeric form.

The results of the coated-wall flow-tube experiments on protein oligomerization are illustrated in Fig. 2. In these experiments, thin protein films were exposed to O_3/NO_2 mixtures. A film thickness of ~ 34 nm, or roughly five layers of BSA, can be calculated assuming an even distribution of the BSA molecules on the inner surface of the glass tube.[20] The experiments were performed at 45% and 96% RH with O_3/NO_2 concentrations of 50/50, 200/50, and 50/200 ppb, respectively. Generally, the reactive sites accessible for oligomerization reactions of the proteins are limited here compared to aqueous solutions, leading to smaller mass fractions of protein oligomers. Furthermore, we observed a 30–40% reduction of the overall oligomer mass fraction (dimer, trimer, and oligomer ≥ 4) compared to similar flow-tube experiments in the absence of NO_2 for comparable RH and O_3 concentrations.[20] Apparently, the lower diffusivity of the proteins in this solid (45% RH) or semi-solid (96% RH) state induces a competition between DTyr and NTyr formation, also indicated by the observation of slower reaction rates for oligomerization in the bulk of the thin protein film compared to its surface.[20,23]

In contrast to the bulk solution experiments, which show a steady increase of the oligomer mass fractions with exposure time, dimer and trimer mass fractions in the flow tube experiments peaked at exposure times of 2–4 h, depending on RH and trace gas concentrations, while only higher oligomers steadily increased over the course of the reaction time (see Fig. 2). This result indicates that as the exposure proceeds, the formation of dimers and trimers becomes slower than their consumption converting them into higher oligomers. The characteristic residence times (lifetimes) of biological particles in the atmosphere can range from hours to weeks, depending on their sizes, aerodynamic, and hygroscopic properties.[32] Our observation indicates that the initial exposure (<2–4 h) of proteins to O_3 and NO_2 mainly leads to the formation of protein dimers and

Faraday Discussions

trimers, and as the exposure proceeds, protein oligomers could be the dominant protein species, *e.g.*, on the surface of bioaerosol particles.

3.2. Protein nitration

Fig. 3 and 4 show the effects of varying NO_2 and O_3 concentrations on the nitration of protein monomers and dimers in homogeneous bulk solution and coated-wall flow-tube experiments, respectively. Exposures were carried out at fixed NO_2 concentrations with varying O_3 concentrations and *vice versa*. The exposure time was varied from 0.5 up to 12 h. While in previous studies total protein nitration degrees (NDs) were investigated upon exposure to O_3 and NO_2,[12,33] we explicitly explored and characterized the reaction kinetics of protein nitration, resolving the individual NDs of the protein monomer and its various oligomers over the course of reaction time.

The results of the bulk solution experiments on protein nitration are illustrated in Fig. 3. The maximum ND of protein monomers and dimers were found to be 7% and 5% after 12 h exposure to 200 ppb O_3 and 50 ppb NO_2, respectively. These results correspond to 1.4 NTyr residues per monomer molecule and 2 NTyr residues per dimer molecule (NTyr/monomer and NTyr/dimer are shown as secondary *y*-axes in Fig. 3 and 4). We found a positive relationship between the NDs and O_3 concentration (Fig. 3a and b), particularly that the increase of O_3 concentration by one order of magnitude from 5 to 50 ppb resulted in an increase of NDs from 4.2 ± 0.2% to 6.9 ± 0.2%, and 2.0 ± 0.3% to 4.5 ± 0.3% after 12 h exposure for the monomer and dimer, respectively. Also, for protein nitration, no significant difference was found when concentrations of NO_2 were varied from 5 to 200 ppb at a fixed O_3 concentration of 50 ppb, as shown in Fig. 3c and d. These results are in accordance with the observations made by Shiraiwa *et al.*[23] on the
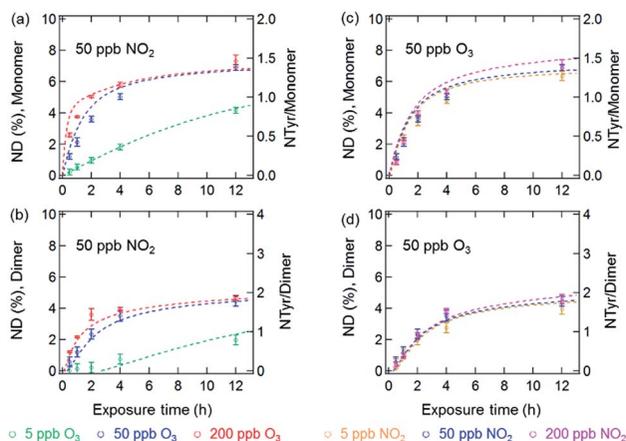

Fig. 3 NDs of protein monomer and dimer (primary *y*-axis), and NTyr number per monomer and dimer (secondary *y*-axis) plotted against reaction time in the aqueous phase reaction of BSA with O_3/NO_2: (a) and (b) at a fixed NO_2 concentration of 50 ppb with varied O_3 concentrations, and (c) and (d) at a fixed O_3 concentration of 50 ppb with varied NO_2 concentrations. The data points and error bars represent the arithmetic mean values and standard deviations of duplicate experiments. The dashed lines are the results of the kinetic model.
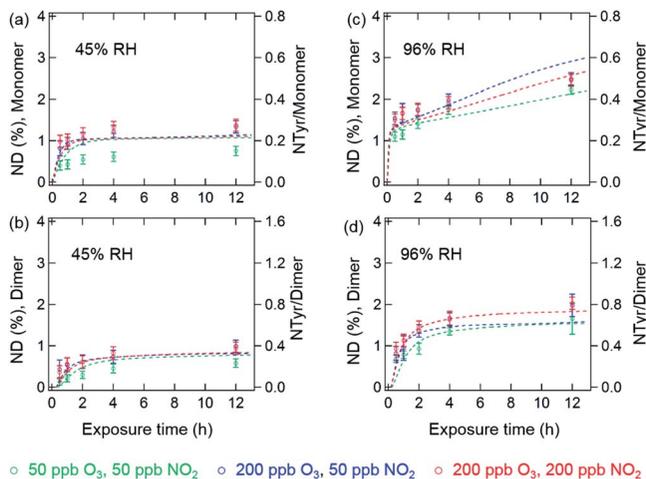
Fig. 4 NDs of protein monomer and dimer (primary y-axis), and NTyr number per monomer and dimer (secondary y-axis) plotted against exposure time upon the exposure of BSA films (thickness 34 nm) to various O_3/NO_2 concentrations: (a) and (b) at 45% RH, and (c) and (d) at 96% RH. The data points and error bars represent the arithmetic mean values and standard deviations of duplicate experiments. The dashed lines are the results of the kinetic model.

study of the reactive uptake of NO_2 by aerosolized proteins. They found that the uptake coefficient of NO_2 (γ_{NO_2}) increased with increasing O_3 concentrations while γ_{NO_2} decreased gradually with increasing NO_2 concentration. Thus, our results confirm that the protein reaction with O_3 and formation of ROI is the rate-limiting step for protein nitration.[21,23] Shiraiwa et al.[23] have excluded NO_3 or N_2O_5 (formed through NO_2 oxidation by O_3) as major contributors to protein nitration. Ghiani et al.[34] reported that nitration of proteins can also occur by nitrate ions in bulk solutions without UV irradiation under acidic conditions (pH < 3 for BSA). The reaction of NO_2 with water can form nitric acid and thereby nitrate ions might appear in the BSA solution. However, we found that the pH of the BSA solutions stayed relatively constant (pH 6.6 ± 0.2; pH meter model WTW multi 350i) for a reaction time of 12 h at 200 ppb NO_2 and 50 ppb O_3, indicating that nitration induced by nitrate ions is likely a minor or negligible pathway in this study. This hypothesis is consistent with the results in Fig. 3c and d that show only a slight increase in ND (monomer, 6.3 ± 0.3% to 6.9 ± 0.2%, and dimer, 4.0 ± 0.3% to 4.5 ± 0.3%, for 12 h reaction) for a one order of magnitude increase in the NO_2 concentration from 5 to 50 ppb.

The results of the temporal increase of NDs of monomer and dimer for reactions of the thin protein films with O_3 and NO_2 concentrations of 50 and 200 ppb at 45% and 96% RH are illustrated in Fig. 4. Here, the NDs for monomer and dimer at 45% RH were found to be around 1% and 0.8% for 12 h exposure, corresponding to 0.2 NTyr/monomer molecule and 0.3 NTyr/dimer molecule. Note that the protein coating consisted of ~5 layers. Therefore, the results likely indicate that on average one Tyr per BSA monomer molecule located on the surface of the protein film was efficiently nitrated, while the bulk nitration occurred at much slower rates. This highly reactive site could be the Tyr residue at

Faraday Discussions

position 161 (Y161), as suggested by Zhang *et al.*[35] The maximum NDs for monomer and dimer reached up to $2.5 \pm 0.1\%$ and $2.0 \pm 0.1\%$ at 96% RH, respectively. However, both of the maximum NDs at 45% and 96% RH were much lower than those obtained for O_3/NO_2 exposure in aqueous solutions (200 ppb O_3 and 50 ppb NO_2). This discrepancy can be explained by a decrease in viscosity and an increase in diffusivity on going from an amorphous solid (45% RH) or semi-solid (96% RH) protein on a coated wall to an aqueous protein solution and was able to be reproduced using a model (see below).[36,37] Furthermore, the NDs of BSA in this study are comparable to those found by Yang *et al.*[33] using the same protein, whereas the nitration efficiency of BSA in general is found to be much lower than the one observed for the major birch pollen allergen Bet v 1 in similar exposure experiments,[12] indicating a strong influence of molecular structure and potentially the amino acid sequence of the reacting protein. From previous mass spectrometric analysis of the site selectivity of protein nitration by O_3/NO_2, it is known that only 3 out of 21 Tyr residues in BSA can be detected in the nitrated form, while in Bet v 1, 4 out of 7 Tyr residues can be nitrated.[12,35] Thus, besides the types of nitrating agents (*e.g.* $ONOO^-$ or O_3/NO_2) and reaction conditions (in aqueous solution or heterogeneous exposure), the nitration efficiency also depends on the fraction of reactive Tyr residues in the investigated protein.

3.3. Kinetics and mechanism of protein nitration and oligomerization by $O_3/$ NO_2

The model results for the reactions of proteins with O_3/NO_2 under the various exposure conditions are shown as the dashed lines in Fig. 1–4. A chemical mechanism involving 19 reactions (see Table S1† for details) was applied in two kinetic models, *i.e.*, a box model for bulk solution experiments and a kinetic multilayer model for aerosol surface and bulk chemistry (KM-SUB)[26] for flow tube
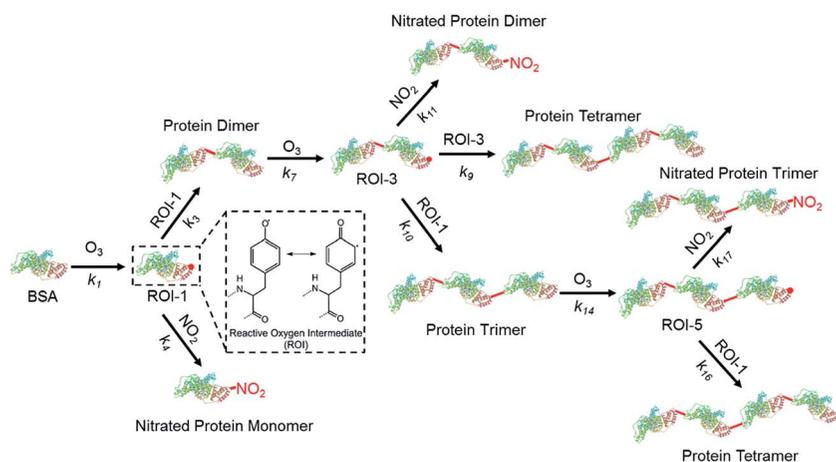

Fig. 5 Schematic overview of the most relevant reactions for protein nitration and oligomerization upon exposure to ozone and nitrogen dioxide. The reactions correspond to protein surface Tyr nitration and oligomerization in the mechanism presented in Table S1.† The molecular structure of the protein (BSA, PDB accession number 3V03) was created using RCSB PDB protein workshop (4.2.0) software.

experiments to fit the experimental data. The most relevant reactions for this mechanism are illustrated in Fig. 5. The first step in the mechanism is the reaction of a Tyr residue with O_3 forming tyrosyl radicals as long-lived reactive oxygen intermediates (ROIs). In the second step of the process, the ROIs can react with each other to form dimers, or with NO_2 to form nitrated monomers. Note that for simplification, each molecule only contains one reactive tyrosine residue, while nitrated and oxidized monomers, dimers and trimers are unable to take part in further reactions in the kinetic model. A dimer can react further with O_3 to form a dimeric ROI, which may react with NO_2 to form a nitrated protein dimer, with monomeric ROI to form a protein trimer or with another dimeric ROI to form a protein tetramer.

The following assumptions were made to enable modelling of the reaction system for bulk solution and coated-wall flow-tube experiments using the sets of physicochemical parameters shown in Table S1 (ESI†): BSA molecules have reactive amino acid residues on their surface (AA1) and in their bulk (AA2), both of them reactive towards O_3. While ROIs formed in the protein bulk can only react with NO_2 to form NTyr, they are unable to form intermolecular DTyr due to steric hindrance.[38] These assumptions were also applied to dimers and trimers. Besides Tyr, O_3 can also oxidize other amino acid residues, *i.e.*, cysteine (Cys), tryptophan (Trp), methionine (Met) and histidine (His).[31] Among them, only Cys is able to cross-link proteins directly upon O_3 exposure, yielding intermolecular disulfide bridges, as one free Cys is available in BSA.[39] This reversible cross-linking mechanism has been shown to be only a minor contributor to protein oligomerization upon O_3/NO_2 exposure previously.[20] The kinetic parameters were obtained using a global optimization method combining a uniformly-sampled Monte Carlo search with a genetic algorithm (MCGA method).[40,41] The genetic algorithm was terminated when the correlation between experimental data and model output reached an optimum. Concentrations of O_3 and NO_2 in the aqueous phase can be estimated using the published Henry's law constant of $K_{sol,cc,O_3} \approx K_{sol,cc,NO_2} \approx 10^{-2}$ M atm^{-1}, which were used as fixed values in the model.[30]

The temporal evolution of NDs and oligomer mass fractions in aqueous solution is well reproduced by the model (Fig. 1 and 3). For the heterogeneous reactions studied in the coated-wall flow-tube experiments at 45% RH and 96% RH, some substantial deviations between modelled and measured data can be observed, and the coefficient of determination (R^2 value) is approximately a factor of two lower than for the aqueous data. For example, the oligomer mass fractions ω at 45% RH in Fig. 2a–d are qualitatively captured fairly well, while the model fails to reproduce their evolution at higher RH, especially for the dimer and trimer (Fig. 2f and g). The observed reduction of dimers in flow tube experiments could be reproduced by the model including the reactions on the surface, where the rates are four orders of magnitude higher than that of bulk reactions. Despite simple model assumptions when describing the complex reaction system that was studied, the model reproduces the experimental data reasonably well with an overall R^2 value of 0.88 for Fig. 1–4. Most of the optimized parameters obtained for the flow tube experiments were close to or the same as those for aqueous solutions (for details see Table S1, ESI†). However, note that some of the rate coefficients would be expected to change as the liquid water content and viscosity varies. Water could actively take part in some of the reactions and its presence at different concentrations could lead to changes in experimental conditions, such

as pH, which would influence the rate of the reactions. As the viscosity increases it is also expected that some rate coefficients would decrease as they become diffusion-limited as per the Smoluchowski diffusion equation.[42,43]

The second-order rate coefficients obtained as model outputs and shown in Table S1† are mostly consistent with previous studies.[20,23] However, as the complex reaction mixture has been reflected in only 19 chemical reactions, the absolute numbers of the rate coefficients obtained for the individual reactions likely do not reflect reality, because further secondary chemistry of various kinds is not included explicitly. It should also be noted that different types of tyrosine residues have not been explicitly included within the model, although these can nitrate at different rates and have different surface accessibilities.[35,44] Neverthe-less, qualitatively, the model results suggest that protein nitration occurs at faster rates than protein oligomerization. The observed and modelled preference of nitration over oligomerization can be rationalized by comparing the mass fraction of nitrated monomer (calculated by multiplying the mass fraction of monomer with NTyr/monomer) with the total oligomer mass fraction. Nitrated monomers were observed to have two times or higher mass fractions compared to all other oligomer mass fractions combined under all experimental conditions. This result indicates that Tyr nitration outcompetes the dimerization/oligomerization process.[22,45]

4. Implications and conclusions

In this study we investigated the kinetics and mechanism of the nitration and oligomerization of proteins induced by O_3 and NO_2 under different atmospheri-cally relevant conditions. We showed the concentration and time dependence of the formation of dimers, trimers and higher protein oligomers as well as their individual nitration degrees. The temporal evolution of the concentrations of these multiple reaction products was well reproduced by a kinetic model with 19 chemical reactions. Protein nitration was found to be kinetically favored over protein oligomerization under the experimental conditions studied in this work. On the basis of the observation that nitrated oligomers formed upon exposure to O_3/NO_2, we suggest further investigation on the allergenic and immunogenic effects by nitrated protein oligomers. The nitrated oligomers were also found in the physiologically-relevant peroxynitrite-induced protein nitration and oligo-merization,[46] for which the mechanism is similar to the one we reported here.[25,47]

The implications of protein chemistry with O_3 and NO_2 under atmospherically relevant conditions are illustrated in Fig. 6. The overall nitration and oligomeri-zation rates were both almost one order of magnitude higher in the aqueous phase than for 45% RH, indicating an increased relevance of the processes under cloud-processing conditions. Also, the yields of protein nitration and oligomeri-zation can be strongly influenced by changes in relative humidity leading to changes of phase states. The protein dimers can yield up to 20% (by mass) for 12 h exposure in the liquid phase and the NDs of monomers and dimers can be up to 7% and 5%, respectively. This result indicates that on average, 1.4 Tyr residues in each monomeric protein molecule and 2 Tyr residues in each dimeric molecule are present in their nitrated forms. For proteins in solid or semi-solid phase states, our measurement and model results suggest that higher protein oligomers are likely to be found at lower RH, e.g., on the surface of bioaerosols, whereas the
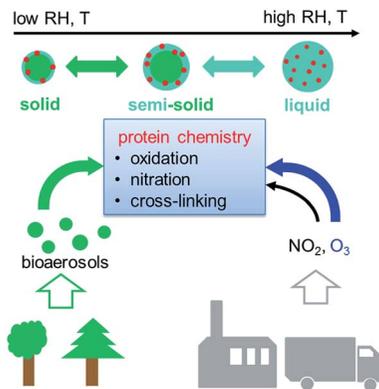
Fig. 6 Atmospheric protein chemistry by ozone (O_3) and nitrogen dioxide (NO_2). Reaction rates are limited by the phase state of proteins and hence the diffusivity of oxidants and protein molecules, which changes with relative humidity (RH) and temperature (T). Air pollutants such as NO_2 and O_3 can enhance allergen release from bioaerosols (*e.g.*, pollen) with O_3 being more important in triggering the nitration, cross-linking and oxidation of allergenic proteins in bioaerosols and other protein-containing particles (*e.g.*, Bet v 1 on urban road dust[15]).

NDs of monomers and dimers remain at ∼1–2%. Using *ab initio* calculations, Sandhiya *et al.*[22] also showed that increased temperature can speed up the formation of tyrosyl radicals by ozonolysis. Thus, it is expected that nitrated and dimeric protein species could be important products of exposure to O_3 and NO_2 under tropical or summer smog conditions. These differences in reaction kinetics should be taken into account in studies on the physiological effects of proteins exposed to anthropogenic air pollutants, as the allergenic proteins in various oligomerization and nitration states might have a different immunogenic potential.

Both increasing levels of O_3 and NO_2 are able to damage pollen grains and facilitate the release of allergens in polluted environments.[3,8,9] However, our results show that the tyrosine nitration and cross-linking of proteins are sensitive towards an increase in O_3 concentration and rather insensitive towards changes in ambient NO_2 concentrations. Therefore, effective control of the enhanced allergenicity induced by air pollutant-modified aeroallergens should point towards the decrease of ambient ozone concentrations.

Acknowledgements

Notes and references

1 M. I. Asher, S. Montefort, B. Björkstén, C. K. Lai, D. P. Strachan, S. K. Weiland, H. Williams and I. P. T. S. Group, *Lancet*, 2006, **368**, 733–743.

2 R. Pawankar, C. E. Baena-Cagnani, J. Bousquet, G. W. Canonica, A. A. Cruz, M. A. Kaliner and B. Q. Lanier, *World Allergy Organ. J.*, 2008, **1**, S4–S17.

3 U. Frank and D. Ernst, *Front. Plant Sci.*, 2016, **7**, 91.

4 K.-H. Kim, S. A. Jahan and E. Kabir, *Environ. Int.*, 2013, **59**, 41–52.

5 U. Pöschl and M. Shiraiwa, *Chem. Rev.*, 2015, **115**, 4440–4475.

6 K. Reinmuth-Selzle, C. J. Kampf, K. Lucas, N. Lang-Yona, J. Fröhlich-Nowoisky, M. Shiraiwa, P. S. J. Lakey, S. Lai, F. Liu, A. T. Kunert, K. Ziegler, F. Shen, R. Sgarbanti, B. Weber, M. G. Weller, I. Bellinghausen, J. Saloga, A. Duschl, D. Schuppan and U. Pöschl, *Environ. Sci. Technol.*, 2017, **51**, 4119–4141.

7 D. Diaz-Sanchez, M. P. Garcia, M. Wang, M. Jyrala and A. Saxon, *J. Allergy Clin. Immunol.*, 1999, **104**, 1183–1188.

8 I. Beck, S. Jochner, S. Gilles, M. McIntyre, J. T. Buters, C. Schmidt-Weber, H. Behrendt, J. Ring, A. Menzel and C. Traidl-Hoffmann, *PLoS One*, 2013, **8**, e80147.

9 Y. Ouyang, Z. Xu, E. Fan, Y. Li and L. Zhang, *Int. Forum. Allergy Rhinol.*, 2016, **6**, 95–100.

10 C. Ackaert, S. Kofler, J. Horejs-Hoeck, N. Zulehner, C. Asam, S. von Grafenstein, J. E. Fuchs, P. Briza, K. R. Liedl and B. Bohle, *PLoS one*, 2014, **9**, e104520.

11 N. Lang-Yona, T. Shuster-Meiseles, Y. Mazar, O. Yarden and Y. Rudich, *Sci. Total Environ.*, 2016, **541**, 365–371.

12 K. Reinmuth-Selzle, C. Ackaert, C. J. Kampf, M. Samonig, M. Shiraiwa, S. Kofler, H. Yang, G. Gadermaier, H. Brandstetter and C. G. Huber, *J. Proteome Res.*, 2014, **13**, 1570–1577.

13 A. D. Estillore, J. V. Trueblood and V. H. Grassian, *Chem. Sci.*, 2016, **7**, 6604–6616.

14 J. Fröhlich-Nowoisky, C. J. Kampf, B. Weber, J. A. Huffman, C. Pöhlker, M. O. Andreae, N. Lang-Yona, S. M. Burrows, S. S. Gunthe, W. Elbert, H. Su, P. Hoor, E. Thines, T. Hoffmann, V. R. Després and U. Pöschl, *Atmos. Res.*, 2016, **182**, 346–376.

15 T. Franze, M. G. Weller, R. Niessner and U. Pöschl, *Environ. Sci. Technol.*, 2005, **39**, 1673–1678.

16 J. T. Buters, A. Kasche, I. Weichenmeier, W. Schober, S. Klaus, C. Traidl-Hoffmann, A. Menzel, J. Huss-Marp, U. Krämer and H. Behrendt, *Int. Arch. Allergy Immunol.*, 2007, **145**, 122–130.

17 F. Liu, S. Lai, K. Reinmuth-Selzle, J. F. Scheel, J. Fröhlich-Nowoisky, V. R. Després, T. Hoffmann, U. Pöschl and C. J. Kampf, *Anal. Bioanal. Chem.*, 2016, **408**, 6337–6348.

18 P. Taylor, R. Flagan, A. Miguel, R. Valenta and M. Glovsky, *Clin. Exp. Allergy*, 2004, **34**, 1591–1596.

19 G. F. Schäppi, P. E. Taylor, I. A. Staff, C. Suphioglu and R. B. Knox, *Sex. Plant Reprod.*, 1997, **10**, 315–323.

20 C. J. Kampf, F. Liu, K. Reinmuth-Selzle, T. Berkemeier, H. Meusel, M. Shiraiwa and U. Pöschl, *Environ. Sci. Technol.*, 2015, **49**, 10859–10866.

21 M. Shiraiwa, Y. Sosedova, A. Rouvière, H. Yang, Y. Zhang, J. P. Abbatt, M. Ammann and U. Pöschl, *Nat. Chem.*, 2011, **3**, 291–295.

22 L. Sandhiya, P. Kolandaivel and K. Senthilkumar, *J. Phys. Chem. B*, 2014, **118**, 3479–3490.

23 M. Shiraiwa, K. Selzle, H. Yang, Y. Sosedova, M. Ammann and U. Pöschl, *Environ. Sci. Technol.*, 2012, **46**, 6672–6680.

24 M. Shiraiwa, K. Selzle and U. Pöschl, *Free Radical Res.*, 2012, **46**, 927–939.

25 S. Pfeiffer, K. Schmidt and B. Mayer, *J. Biol. Chem.*, 2000, **275**, 6346–6352.

26 M. Shiraiwa, C. Pfrang and U. Pöschl, *Atmos. Chem. Phys.*, 2010, **10**, 3673–3691.

27 G. Li, H. Su, X. Li, U. Kuhn, H. Meusel, T. Hoffmann, M. Ammann, U. Pöschl, M. Shao and Y. Cheng, *Atmos. Chem. Phys.*, 2016, **16**, 10299–10311.

28 F. Liu, K. Reinmuth-Selzle, S. Lai, M. G. Weller, U. Pöschl and C. J. Kampf, *J. Chromatogr. A*, 2017, **1495**, 76–82.

29 S. L. Ellison, M. Rosslein and A. Williams, in *Quantifying uncertainty in analytical measurement*, Eurachem, 2000.

30 R. Sander, *Atmos. Chem. Phys.*, 2015, **15**, 4399–4981.

31 V. K. Sharma and N. J. Graham, *Ozone: Sci. Eng.*, 2010, **32**, 81–90.

32 V. R. Després, J. A. Huffman, S. M. Burrows, C. Hoose, A. S. Safatov, G. Buryak, J. Fröhlich-Nowoisky, W. Elbert, M. O. Andreae, U. Pöschl and R. Jaenicke, *Tellus, Ser. B*, 2012, **64**, 1–58.

33 H. Yang, Y. Zhang and U. Pöschl, *Anal. Bioanal. Chem.*, 2010, **397**, 879–886.

34 A. Ghiani, M. Bruschi, S. Citterio, E. Bolzacchini, L. Ferrero, G. Sangiorgi, R. Asero and M. G. Perrone, *Sci. Total Environ.*, 2016, **573**, 1589–1597.

35 Y. Zhang, H. Yang and U. Pöschl, *Anal. Bioanal. Chem.*, 2011, **399**, 459–471.

36 M. Shiraiwa, M. Ammann, T. Koop and U. Pöschl, *Proc. Natl. Acad. Sci. U. S. A.*, 2011, **108**, 11003–11008.

37 E. Mikhailov, S. Vlasenko, S. Martin, T. Koop and U. Pöschl, *Atmos. Chem. Phys.*, 2009, **9**, 9491–9522.

38 W. H. Heijnis, H. L. Dekker, L. J. de Koning, P. A. Wierenga, A. H. Westphal, C. G. de Koster, H. Gruppen and W. J. van Berkel, *J. Agric. Food Chem.*, 2010, **59**, 444–449.

39 T. Ueki, Y. Hiragi, M. Kataoka, Y. Inoko, Y. Amemiya, Y. Izumi, H. Tagawa and Y. Muroga, *Biophys. Chem.*, 1985, **23**, 115–124.

40 T. Berkemeier, S. S. Steimer, U. K. Krieger, T. Peter, U. Pöschl, M. Ammann and M. Shiraiwa, *Phys. Chem. Chem. Phys.*, 2016, **18**, 12662–12674.

41 A. M. Arangio, J. H. Slade, T. Berkemeier, U. Pöschl, D. A. Knopf and M. Shiraiwa, *J. Phys. Chem. A*, 2015, **119**, 4533–4544.

42 W. Scheider, *J. Phys. Chem.*, 1972, **76**, 349–361.

43 L. J. Lapidus, W. A. Eaton and J. Hofrichter, *Proc. Natl. Acad. Sci. U. S. A.*, 2000, **97**, 7220–7225.

44 B. Petersen, T. N. Petersen, P. Andersen, M. Nielsen and C. Lundegaard, *BMC Struct. Biol.*, 2009, **9**, 1.

45 J. M. Souza, G. Peluffo and R. Radi, *Free Radical Biol. Med.*, 2008, **45**, 357–366.

46 Y. J. Zhang, Y. F. Xu, X. Q. Chen, X. C. Wang and J.-Z. Wang, *FEBS Lett.*, 2005, **579**, 2421–2427.

47 R. Radi, *Proc. Natl. Acad. Sci. U. S. A.*, 2004, **101**, 4003–4008.